Available online at www.sciencedirect.com
SCIENCE DIRECT®
Biochemical and Biophysical Research Communications 330 (2005) 60–64
BBRC
www.elsevier.com/locate/ybbrc

Sulfur K-edge X-ray absorption spectroscopy as an experimental probe for *S*-nitroso proteins

Robert K. Szilagyi *, David E. Schwab

Department of Chemistry and Biochemistry, Montana State University, Bozeman, MT 59717, USA

Received 25 January 2005

Abstract

X-ray absorption spectroscopy at the sulfur K-edge (2.4–2.6 keV) provides a sensitive and specific technique to identify *S*-nitroso compounds, which have significance in nitric oxide-based cell signaling. Unique spectral features clearly distinguish the *S*-nitroso-form of a cysteine residue from the sulfhydryl-form or from a methionine thioether. Comparison of the sulfur K-edge spectra of thiolate, thiol, thioether, and *S*-nitroso thiolate compounds indicates high sensitivity of energy positions and intensities of XAS pre-edge features as determined by the electronic environment of the sulfur absorber. A new experimental setup is being developed for reaching the in vivo concentration range of *S*-nitroso thiol levels in biological samples.

Keywords: Nitric oxide; *S*-Nitroso proteins; Hemoglobin; X-ray absorption spectroscopy; Electronic structure

Nitric oxide (NO) is a free radical that is implicated in the regulation of blood circulation [1,2], cell death [3,4], and neural functions [5,6]. The proposed mechanism for NO bioactivity involves post-translational modifications, where NO can oxidize proteins or attach NO_2 (nitrate) or NO (nitrosate) to amino acid residues [1–7]. The S-nitrosation of specific cysteines is emerging as an important mechanism for regulation of signal transduction in cells [8]. Despite the progress in understanding the details of NO-based cell signaling, research is hindered by a lack of a sensitive and specific method to identify S-nitrosated (SNO) proteins [9,10]. This is partially due to the low concentration of nitrosated intracellular proteins as well as the great sensitivity of the ON–S bond to sample aging, manipulation, and redox conditions [11,12].

In red blood cells, release of NO from a specific cysteine (SNO-βC93) induced by hypoxic conditions (low tissue pO_2) triggers vasodilation [2]. At physiological conditions [13,14], the hemoglobin concentration is in the millimolar range. It is proposed, however, that only 1 in 5000 hemoglobin possess a molecule of NO (micromolar range) [15].

The current chemical [11,16–19], electrochemical [20], biochemical techniques [10,21–23], and standards [24] employed in detecting and quantitating protein SNO levels at an uncomfortable low analyte concentration utilize the *unique chemical reactivity* of NO. Among the spectroscopic methods, the EPR technique can determine the metal (heme) bound NO at nanomolar level [25–27]; however, it is transparent to SNO due to its diamagnetic electronic ground state.

The *unique electronic structure* of *S*-nitroso thiols can provide a specific experimental handle for detecting and characterizing SNO formation and release. Molecular orbital theory defines σ and π bonding interactions between the sulfur 3p and the NO π* orbitals that render the SNO electronic structure unique with respect to cysteine and methionine. Fig. 1 illustrates the three lowest

* Corresponding author. Fax: +1 406 994 5407.
E-mail address: Szilagyi@Montana.EDU (R.K. Szilagyi).

0006-291X/$ - see front matter © 2005 Elsevier Inc. All rights reserved.
doi:10.1016/j.bbrc.2005.02.127

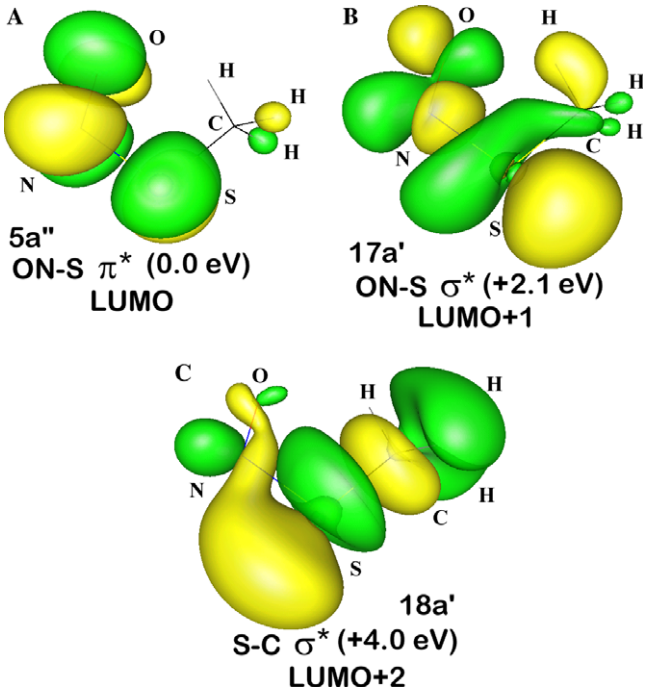

Fig. 1. Frontier unoccupied orbitals (LUMO through LUMO + 2) of *S*-nitroso methylthiolate (H_3C-SNO).

lying, unoccupied orbitals in the order of increasing energy with significant sulfur character. The sensitivity of SNO toward reduction can be rationalized by the antibonding nature of these valence orbitals along the N–S bond vectors.

The sulfur 3p-based bonding interactions of SNO can be directly probed by X-ray absorption spectroscopy [28]. The sulfur K-edge XAS in the energy range of 2.4–2.6 keV corresponds to excitation of sulfur core 1s electrons to unoccupied orbitals, giving various bound states and, at higher energies, excitation to the continuum giving rise to an intense edge jump. The bound states appear as pre-edge or rising-edge features before the edge jump. Analysis of these near-edge spectral features (NEXAS [29]) provides electronic structural information about the absorber atom, while the energy region beyond the edge jump (EXAFS [30]) gives geometric information by defining the radial distribution of atoms (as scatterers) around the absorber. Since the bound state transitions are localized on sulfur and electric dipole allowed, the intensity of the pre-edge features is proportional to the sulfur 3p character in the unoccupied, acceptor orbitals.

Sulfur K-edge XAS has already been successfully applied in analytical determination of chemical speciation [31–38] and in electronic structure studies of transition metal thiolates [39,40], Fe–S clusters [41,42], and various bioinorganic active sites [28,43–45]. This study introduces a novel experimental way of detecting SNO in proteins using a comparison of sulfur K-edge XAS spectra of *S*-nitroso compounds to cysteine and methionine, and various thiolate salts. Using the data obtained for the solid models, the spectrum of the crystallographically characterized *S*-nitroso human hemoglobin [46] is predicted.

Materials and methods

XAS data collection. SNO compounds (Fig. S1) were purchased from Cayman Chemicals and other sulfur compounds from Sigma–Aldrich. Sulfur K-edge XAS measurements were carried out at BL9.3.1 of Advanced Light Source under ultrahigh vacuum (10^{-7} torr) with a liquid nitrogen-cooled sample rod. The solid samples were ground and pasted onto a sulfur-free Mylar dot (Shercon). Preparation of SNO samples was carried out in a liquid nitrogen boil-off cooled, portable glovebox with continuous dry nitrogen purge (atmosphere temperature was maintained at 0 ± 5 °C) to minimize SNO decomposition. Due to the low temperature data collection setup, no photoreduction, radiation damage or change in the color of the samples was observed over a lengthy exposure to the beam. The sample cell was positioned at approximately 45° relative to the incident beam. Fluorescence signal was collected using a Si-photodiode aligned parallel with the sample cell. The incident photon energy was scanned in 0.5 eV steps outside the rising-edge region, where the stepsize was 0.1 eV. The resting time of the Si(1 1 1) double crystal monochromator and the dwell time for data collection were set to 400 ms and 1s, respectively. At least five scans were averaged to obtain a good signal-to-noise ratio. The incident photon energy was calibrated to the first transition (2472.02 eV) of the sodium thiolsulfate pentahydrate spectrum with reproducibility within 0.1 eV. A smooth background (second order polynomial) was subtracted from the spectra and normalized at 2490 eV of the spline (second order polynomial). Rough data processing was carried out at the beamline immediately after data collection, while final data processing of calibration, background subtraction, spline, and fitting was performed using PeakFit 4.12 (SeaSolve).

Electronic structure calculations. Electronic structure calculations were carried out using the Gaussian03 suite [47]. The geometry of *S*-nitroso methylthiolate was optimized using GGA Becke exchange [48] and Perdew correlation [49] functionals with 6-31G(d) basis set for all atoms [50,51]. The electronic wave function at the equilibrium geometry (no imaginary vibrational frequency) was analyzed by Natural Population Analysis [52–54].

Results and discussion

Unique spectral features of SNO

The sulfur K-edge spectra (Fig. 2) of sodium salt, sulfhydryl, and *S*-nitroso thiolates show dramatic XAS spectral differences. The thiolate salt has a characteristic transition at 2472.1 eV, which is well resolved from the rising-edge features. The former transition corresponds to a sulfur 1s → S–C σ* excitation, while the latter to →sulfur 4p excitations superimposed with atomic scattering. In cysteine, the protonation of sulfur increases the sulfur effective nuclear charge and thus shifts the →C–S σ* excitation to higher energy (2474.2 eV). The corresponding feature in *S*-nitroso glutathione (GSNO, Fig. S1) appears at even higher energy (2474.9 eV), due

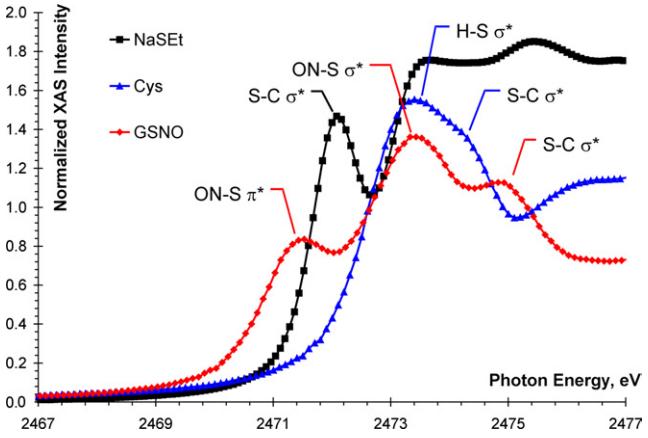

Fig. 2. Normalized sulfur K-edge spectra of sodium ethylthiolate (black ■), cysteine (blue ▲), and GSNO (red ♦) with spectral assignments. (For interpretation of the references to color in this figure legend, the reader is referred to the web version of this paper.)

to electron donation from the sulfur 3p orbital to a vacant π* orbital of the formally NO^+ moiety. As anticipated from Fig. 1, NO^+ binding to the thiolate gives rise to features corresponding to →ON–S π* and σ* excitations, at 2471.4 and 2473.3 eV, respectively (Fig. 2). The energy splitting of the three resolved features (1.9 and 1.5 eV for ON–S π*/σ* and ON–S/S–C σ*, respectively) of the GSNO spectrum correlates well with the calculated splitting of the unoccupied orbitals (2.1 and 1.9 eV, respectively) in the ground electronic state of *S*-nitroso methylthiolate shown in Fig. 1.

Sensitivity of sulfur K-edge XAS

In addition to detecting SNO, sulfur K-edge XAS shows sensitivity to changes in the electronic environment of the sulfur absorber. Perturbation in the electron donating ability of the organic moiety changes the energy positions of pre-edge features by affecting the sulfur effective nuclear charge. For example, the S–C σ* transition is shifted up in energy by approximately 0.8 eV in the sodium salt of phenylthiolate (Table 1) due to the electron withdrawing effect of the aromatic ring, relative to the alkyl groups in ethylthiolate (Fig. S2). In methionine, two C–S σ* transitions are observed, which are only slightly higher in energy (0.1–0.2 eV) relative to cysteine (Fig. S3). Most importantly in SNO, the perturbation of the organic moiety influences the ON–S bonding, as indicated by the change in energy positions of corresponding features (Table 1, Fig. S4) in *N*-acetyloxy-3-nitrosothiovaline (Fig. S1, SNAP) relative to GSNO. In SNAP, the sulfur is attached to a tertiary carbon, which has a greater electron donating ability than the primary carbon in GSNO (or SNO-Cys). This results in increased electron donation to the sulfur (decreasing effective nuclear charge) and thus shifts the transitions corresponding to the C–S σ* excitation down in energy by about 0.7 eV (Table 1). It is important to note that the ON–S σ bonding interaction is also perturbed, while the perpendicular ON–S π bonding does not seem to be affected significantly, as indicated by the energy positions of corresponding transitions in Table 1.

Table 1
Assignments of sulfur 1s core electron excitations for selected model compounds

Compounds	Excitation (S 1s→)	Transition energy (eV)
NaSEt	S–C σ*	2472.1
NaSPh	S–C σ*	2472.9
Cysteine	H–S σ*	2473.4
	S–C σ*	2474.2
Methionine	S–C σ*	2473.5
		2474.4
GSNO	ON–S π*	2471.4
	ON–S σ*	2473.3
	S–C σ*	2474.9
SNAP	ON–S π*	2471.3
	ON–S σ*	2472.9
	S–C σ*	2474.2

Predicted spectrum for S-nitroso human hemoglobin

Using the normalized sulfur K-edge spectra of GSNO, cysteine, and methionine, the XAS spectra of *S*-nitroso proteins can be predicted. The tetrameric, *S*-nitroso hemoglobin [46] contains 12 sulfur atoms that are potential absorbers in sulfur XAS. Subunits A and C contribute Met32, Met76, and Cys104, while subunits B and D give rise to features due to Met55, Cys112, and SNO-Cys93. The heme bound NO will not contribute to the XAS spectrum in this energy region.

The predicted sulfur K-edge spectrum of the *S*-nitroso hemoglobin is shown in Fig. 3. Due to the overlapping features, only the sulfur 1s → ON–S π* transition is expected to be resolved in the protein spectra. *The minimum at 2471.4 ± 0.1 eV of the second derivative spectrum (dotted lines) allows for the quantitation of the*

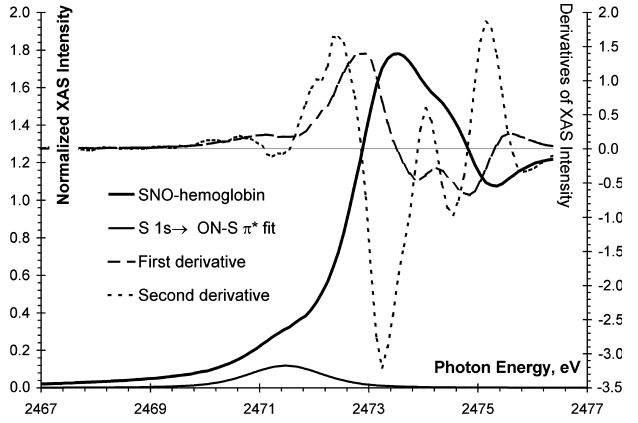

Fig. 3. Predicted sulfur K-edge spectrum of the S-nitrosated-form of human hemoglobin.

ON–S π transition, which can be directly correlated with the S-nitroso thiol concentration*. Alternatively, subtraction of protein spectra with and without bound SNO can give resolved features corresponding to the ON–S π* and σ* transitions, thus providing two points for analytical quantitation.

The potential of XAS has been demonstrated for detecting *S*-nitroso compounds. The high sensitivity of sulfur K-edge XAS provides insights into the electronic, electrostatic, and steric environments around the SNO moiety. These can be derived from pre-edge energy positions, intensities and from EXAFS analysis, respectively. Experiments carried out at Advanced Light Source BL9.3.1 employ fluorescence detection in an ultrahigh vacuum chamber. In order to approach the concentration range of in vivo samples, a new beamline end-station is being designed with detectors for simultaneous data collection in transmission, electron-yield, and fluorescence modes from windowless, frozen biological samples.

Acknowledgments

Authors are thankful for financial support from NSF EPSCoR (Infrastructure: Cross-Sectional Partnership Building for the Future) and NIH BRIN P20 RR-16455-01, for stimulating discussions with Profs. D.A. Singel and E.A. Dratz, and for assistance from ALS staff. D.E.S. acknowledges the graduate student fellowship from NIH BRIN. We also thank A.S. Schlachter (ALS, LBNL) for his assistance with data collection and arrangement of the beam time. The Advanced Light Source is supported by the Director, Office of Energy Research, Office of Basic Energy Sciences, Materials Sciences Division of the US Department of Energy under contract No. DE-AC03-76SF00098.

Appendix A. Supplementary data

Supplementary data associated with this article can be found, in the online version, at doi:10.1016/j.bbrc.2005.02.127.

References

[1] J.S. Stamler, D.I. Simon, O. Jaraki, J.A. Osborne, S. Francis, M. Mullins, D. Singel, J. Loscalzo, S-nitrosylation of tissue-type plasminogen-activator confers vasodilatory and antiplatelet properties on the enzyme, Proc. Natl. Acad. Sci. USA 89 (1992) 8087–8091.

[2] J.S. Stamler, G. Meissner, Physiology of nitric oxide in skeletal muscle, Phys. Rev. 81 (2001) 209–237.

[3] C.M. Schonhoff, B. Gaston, J.B. Mannick, Nitrosylation of cytochrome *c* during apoptosis, J. Biol. Chem. 278 (2003) 18265–18270.

[4] J.Y. Heo, S.L. Campbell, Mechanism of p21(Ras) *S*-nitrosylation and kinetics of nitric oxide-mediated guanine nucleotide exchange, Biochemistry 43 (2004) 2314–2322.

[5] S.A. Lipton, J.S. Stamler, Actions of redox-related congeners of nitric-oxide at the NMDA receptor, Neuropharm 33 (1994) 1229–1233.

[6] S.A. Lipton, Y.B. Choi, H. Takahashi, D.X. Zhang, W.Z. Li, A. Godzik, L.A. Bankston, Cysteine regulation of protein function—as exemplified by NMDA-receptor modulation, Trends Neurosci. 25 (2002) 474–480.

[7] J.S. Stamler, A. Hauslade, Oxidative modifications in nitrosative stress, Nat. Struct. Biol. 5 (1998) 247–249.

[8] P. Lane, S.S. Gross, Cell signaling by nitric oxide, Semin. Nephrol. 19 (1999) 215–229.

[9] J.B. Mannick, C.M. Schonhoff, NO means no and yes: regulation of cell signaling by protein nitrosylation, Free Rad. Res. 38 (2004) 1–7.

[10] S.R. Jaffrey, M. Fang, S.H. Snyder, Nitrosopeptide mapping: a novel methodology reveals S-nitrosylation of Dexras1 on a single cysteine residue, Chem. Biol. 9 (2002) 1329–1335.

[11] E. Nagababu, S. Ramasamy, D.R. Abernethy, J.M. Rifkind, Active nitric oxide produced in the red cell under hypoxic conditions by deoxyhemoglobin-mediated nitrite reduction, J. Biol. Chem. 278 (2003) 46349–46356.

[12] T. Rassaf, N.S. Bryan, R.E. Maloney, V. Specian, M. Kelm, NO adducts in mammalian red blood cells: too much or too little?, Nat. Med. 9 (2003) 481–482.

[13] R.J. Gorczynski, B.R. Duling, Role of oxygen in arteriolar functional vasodilation in hamster striated muscle, Am. J. Physiol. 235 (1978) H505–H515.

[14] C.R. Honig, T.E. Gayeski, Resistance to O_2 diffusion in anemic red muscle: roles of flux density to cell pO_2, Am. J. Physiol. 265 (1993) H868–H875.

[15] D.J. Singel, J.S. Stamler, Chemical physiology of blood flow regulation by red blood cells: role of nitric oxide and snohemoglobin, Annu. Rev. Physiol. 67 (2005) 99–145.

[16] J.B. Mannick, A. Hausladen, L.M. Liu, D.T. Hess, M. Zeng, Q.X. Miao, L.S. Kane, A.J. Gow, J.S. Stamler, Fas-induced caspase denitrosylation, Science 284 (1999) 651–654.

[17] J.P. Eu, J.H. Sun, L. Xu, J.S. Stamler, G. Meissner, The skeletal muscle calcium release channel: coupled O_2 sensor and NO signaling functions, Cell 102 (2000) 499–509.

[18] R. Marley, M. Feelisch, S. Holt, K. Moore, A chemiluminescence-based assay for *S*-nitrosoalbumin and other plasma *S*-nitrosothiols, Free Rad. Res. 32 (2000) 1–9.

[19] T.J. McMahon, R.E. Moon, B.P. Luchsinger, M.S. Carraway, A.E. Stone, B.W. Stolp, A.J. Gow, J.R. Pawloski, P. Watke, D.J. Singel, C.A. Piantadosi, J.S. Stamler, Nitric oxide in the human respiratory cycle, Nat. Med. 8 (2002) 711–717.

[20] B. Datta, T. Tufnell-Barrett, R.A. Bleasdale, C.J. Jones, I. Beeton, Red blood cell nitric oxide as an endocrine vasoregulator: a potential role in congestive heart failure, Circulation 109 (2004) 1339–1342.

[21] J.S. Stamler, D.T. Hess, D.J. Singel, Reply to "NO adducts in mammalian red blood cells: too much or too little?", Nat. Med. 9 (2003) 483–484.

[22] B. Gaston, S. Sears, J. Woods, J. Hunt, M. Ponaman, T. McMahon, J.S. Stamler, Bronchodilator *S*-nitrosothiol deficiency in asthmatic respiratory failure, Lancet 351 (1998) 1317–1319.

[23] B. Gaston, J. Reilly, J.M. Drazen, J. Fackler, P. Ramdev, D. Arnelle, M.E. Mullins, D.J. Sugarbaker, C. Chee, D.J. Singel, J. Loscalzo, J.S. Stamler, Endogeneous nitrogen oxides and bronchodilator *S*-nitrosothiols in human airways, Proc. Natl. Acad. Sci. USA 90 (1993) 10957–10961.

[24] J.S. Stamler, *S*-Nitrosothiols in the blood: roles, amounts and methods of analysis, Circ. Res. 94 (2004) 414–417.

[25] A.B. Milsom, C.J. Jones, J. Goodfellow, M.P. Frenneaux, J.R. Peters, P.E. James, Abnormal metabolic fate of nitric oxide in type I diabetes mellitus, Diabetologia 45 (2002) 1515–1522.
[26] K. Kirima, K. Tsuchiya, H. Sei, T. Hasegawa, M. Shikishima, Evaluation of systemic blood NO dynamics by EPR spectroscopy: HbNO as an endogenous index of NO, Am. J. Physiol. Heart Circ. Physiol. 285 (2003) H589–H596.
[27] G. Aldini, M. Orioli, R. Maffei Facino, M. Giovanna Clement, M. Albertini, Nitrosohemoglobin formation after infusion of NO solutions: ESR studies in pigs, Biochem. Biophys. Res. Commun. 318 (2004) 405–414.
[28] S.E. Shadle, J.E. Penner-Hahn, H.J. Schugar, B. Hedman, K.O. Hodgson, E.I. Solomon, X-ray absorption spectroscopic studies of the blue copper site: metal and ligand K-edge studies to probe the origin of the EPR hyperfine splitting in plastocyanin, J. Am. Chem. Soc. 115 (1993) 767–776.
[29] E.I. Solomon, B. Hedman, K.O. Hodgson, A. Dey, R.K. Szilagyi, Ligand K-edge X-ray absorption spectroscopy: covalency of ligand–metal bonds, Coord. Chem. Rev. 249 (2004) 97–129.
[30] H.H. Zhang, B. Hedman, K.E. Hodgson, in: E.I. Solomon, A.B.P. Lever (Eds.), Inorganic Electronic Structure and Spectroscopy, Wiley, New York, 1999, pp. 513–554.
[31] A. Rompel, R.M. Cinco, M.J. Latimer, A.E. McDermott, R.D. Guiles, A. Quintanilha, R.M. Krauss, K. Sauer, V.K. Yachandra, M.P. Klein, Sulfur K-edge X-ray absorption spectroscopy: a spectroscopic tool to examine the redox state of S-containing metabolites in vivo, Proc. Natl. Acad. Sci. USA 95 (1998) 6122–6127.
[32] E. Paris, G. Giuli, M.R. Carroll, I. Davoli, The valence and speciation of sulfur in glasses by X-ray absorption spectroscopy, Can. Mineral. 39 (2001) 331–339.
[33] D.A. McKeown, I.S. Muller, H. Gan, I.L. Pegg, W.C. Stolte, Determination of sulfur environments in borosilicate waste glasses using X-ray absorption near-edge spectroscopy, J. Non-Cryst. Solids 333 (2004) 74–84.
[34] I.J. Pickering, G.N. George, E.Y. Yu, D.C. Brune, C. Tuschak, J. Overmann, J.T. Beatty, R.C. Prince, Analysis of sulfur biochemistry of sulfur bacteria using X-ray absorption spectroscopy, Biochemistry 40 (2001) 8138–8145.
[35] A. Prange, R. Chauvistre, H. Modrow, J. Hormes, H.G. Truper, C. Dahl, Quantitative speciation of sulfur in bacterial sulfur globules: X-ray absorption spectroscopy reveals at least three different species of sulfur, Microbiology-Sgm 148 (2002) 267–276.
[36] M. Sandstrom, F. Jalilehvand, I. Persson, U. Gelius, P. Frank, I. Hall-Roth, Deterioration of the seventeenth-century warship Vasa by internal formation of sulphuric acid, Nature 415 (2002) 893–897.
[37] E.Y. Sneeden, H.H. Harris, I.J. Pickering, R.C. Prince, S. Johnson, X.J. Li, E. Block, G.N. George, The sulfur chemistry of shiitake mushroom, J. Am. Chem. Soc. 126 (2004) 458–459.
[38] D. Solomon, J. Lehmann, C.E. Martinez, Sulfur K-edge XANES spectroscopy as a tool for understanding sulfur dynamics in soil organic matter, Soil Sci. Soc. Am. J. 67 (2003) 1721–1731.
[39] S.E. Shadle, B. Hedman, K.O. Hodgson, E.I. Solomon, Ligand K-edge X-Ray-absorption spectroscopic studies: metal–ligand covalency in a series of transition-metal tetrachlorides, J. Am. Chem. Soc. 117 (1995) 2259–2272.
[40] K.R. Williams, B. Hedman, K.O. Hodgson, E.I. Solomon, Ligand K-edge X-ray absorption spectroscopic studies: metal–ligand covalency in transition metal tetrathiolates, Inorg. Chim. Acta 263 (1997) 315–321.
[41] T. Glaser, B. Hedman, K.O. Hodgson, E.I. Solomon, Ligand K-Edge X-ray absorption spectroscopy: a direct probe of ligand–metal covalency, Acc. Chem. Res. 33 (2000) 859–868.
[42] A. Dey, T. Glaser, M.M.J. Couture, L.D. Eltis, R.H. Holm, B. Hedman, K.O. Hodgson, E.I. Solomon, Ligand K-edge X-ray absorption spectroscopy of $[Fe_4S_4]^{(1+,2+,3+)}$ clusters: changes in bonding and electronic relaxation upon redox, J. Am. Chem. Soc. 126 (2004) 8320–8328.
[43] K. Rose, S.E. Shadle, M.K. Eidsness, D.M. Kurtz, R.A. Scott, B. Hedman, K.O. Hodgson, E.I. Solomon, Investigation of iron–sulfur covalency in rubredoxins and a model system using sulfur K-edge X-ray absorption spectroscopy, J. Am. Chem. Soc. 120 (1998) 10743–10747.
[44] S. DeBeer George, M. Metz, R.K. Szilagyi, H. Wang, S.P. Cramer, Y. Lu, W.B. Tolman, B. Hedman, K.O. Hodgson, E.I. Solomon, A quantitative description of the ground-state wave function of Cu_A by X-ray absorption spectroscopy: comparison to plastocyanin and relevance to electron transfer, J. Am. Chem. Soc. 123 (2001) 5757–5767.
[45] S. DeBeer George, L. Basumallick, R.K. Szilagyi, D.W. Randall, M.G. Hill, A.M. Nersissian, J.S. Valentine, B. Hedman, K.O. Hodgson, E.I. Solomon, Spectroscopic investigation of stellacyanin mutants: axial ligand interactions at the blue copper site, J. Am. Chem. Soc. 125 (2003) 11314–11328.
[46] N.L. Chan, P.H. Rogers, A. Arnone, Crystal structure of the *S*-nitroso form of liganded human hemoglobin, Biochemistry 37 (1998) 16459–16464.
[47] M.J. Frisch, G.W. Trucks, H.B. Schlegel, G.E. Scuseria, M.A. Robb, J.R. Cheeseman, J.A. Montgomery, Jr., T. Vreven, K.N. Kudin, J.C. Burant, J.M. Millam, S.S. Iyengar, J. Tomasi, V. Barone, B. Mennucci, M. Cossi, G. Scalmani, N. Rega, G.A. Petersson, H. Nakatsuji, M. Hada, M. Ehara, K. Toyota, R. Fukuda, J. Hasegawa, M. Ishida, T. Nakajima, Y. Honda, O. Kitao, H. Nakai, M. Klene, X. Li, J.E. Knox, H.P. Hratchian, J.B. Cross, C. Adamo, J. Jaramillo, R. Gomperts, R.E. Stratmann, O. Yazyev, A.J. Austin, R. Cammi, C. Pomelli, J.W. Ochterski, P.Y. Ayala, K. Morokuma G.A. Voth, P. Salvador, J.J. Dannenberg, V.G. Zakrzewski, S. Dapprich, A.D. Daniels, M.C. Strain, O. Farkas, D.K. Malick, A.D. Rabuck, K. Raghavachari, J.B. Foresman, J.V. Ortiz, Q. Cui, A.G. Baboul, S. Clifford, J. Cioslowski, B.B. Stefanov, G. Liu, A. Liashenko, P. Piskorz, I. Komaromi, R.L. Martin, D.J. Fox, T. Keith, M.A. Al-Laham, C.Y. Peng, A. Nanayakkara, M. Challacombe, P.M.W. Gill, B. Johnson, W. Chen, M.W. Wong, C. Gonzalez, J.A. Pople, Gaussian03 Rev. C 02, Gaussian, Inc., Pittsburgh, PA, 2004.
[48] A.D. Becke, Density-functional exchange-energy approximation with correct asymptotic behavior, Phys. Rev. A 38 (1988) 3098–3100.
[49] J.P. Perdew, Density-functional approximation for the correlation energy of the inhomogeneous electron gas, Phys. Rev. B 33 (1986) 8822–8824.
[50] M.M. Francl, W.J. Pietro, W.J. Hehre, J.S. Binkley, M.S. Gordon, D.J. DeFrees, J.A. Pople, Self-consistent molecular orbital methods. XXIII. A polarization-type basis set for second-row elements, J. Chem. Phys. 77 (1982) 3654–3665.
[51] V.A. Rassolov, J.A. Pople, M.A. Ratner, T.L. Windus, 6-31G* basis set for atoms K through Zn, J. Chem. Phys. 109 (1998) 1223–1229.
[52] J.P. Foster, F. Weinhold, Natural hybrid orbitals, J. Am. Chem. Soc. 102 (1980) 7211–7218.
[53] J.E. Carpenter, F. Weinhold, Analysis of the geometry of the hydroxymethyl radical by the "different hybrids for different spins" natural bond orbital procedure, J. Mol. Struct. (THEOCHEM) 46 (1988) 41–62.
[54] A.E. Reed, L.A. Curtiss, F. Weinhold, Intermolecular interactions from a natural bond orbital, donor–acceptor viewpoint, Chem. Rev. 88 (1988) 899–926.